Simple Polymerization Through Oxygen at Reduced Volumes using Oil and Water.

Kevin M. Burridge[†], Nethmi De Alwis Watuthanthrige[†], Camryn Payne, Richard C. Page, Dominik Konkolewicz*

Department of Chemistry and Biochemistry, Miami University, 651 E High St, Oxford, OH, 45056, USA

[†] Denotes equal authorship

* Correspondence: d.konkolewicz@miamiOH.edu

Abstract

An enduring question is: what is the simplest and easiest way to obtain tailored polymers? This communication explores a robust photoiniferter polymerization with only two active ingredients that requires no prior deoxygenation and can be performed on the milliliter scale or sub-milliliter scale. Rather than leaving headspace in the polymerization vessel or scaling reactions up to fill the vessel, this approach fills the headspace of the reaction vessel with mineral oil or inert solvents. This approach can also be applied to polar monomers in aqueous media, using oil as the inert solvent, or to hydrophobic monomers with water as the inert solvent. This method removes enough ambient oxygen that the photoiniferter reaction proceeds with no deoxygenation step, and achieves high conversion and good molecular weight control in 10-20 hours in both aqueous and organic solvents. Complex polymer architectures such as multiblock copolymers and gradient polymers were successfully synthesized by this approach.

Introduction

Due to the triplet ground state of oxygen, radical reactions are sensitive to irreversible termination in the presence of oxygen. Reversible deactivation radical polymerization methods[1] such as atom transfer radical polymerization (ATRP)[2–5] and reversible addition-fragmentation chain transfer (RAFT)[6,7,16–19,8–15] polymerization are also sensitive to oxygen, often requiring 15 minutes of inert-gas sparging to remove oxygen. Other measures such as longer sparging times, freeze-pump-thaw, inhibitor removal, and specialized glassware like Schlenk flasks may be required. For standard milliliter to liter scale reactions, these methods are practical. However, libraries of polymers that can be synthesized quickly and on reasonably small (milliliter to microliter) scales are difficult or impossible to access using conventional methods of deoxygenation.[20] Synthesis of such libraries of complex polymers is desirable to access highly functional polymeric materials for pharmaceutical applications.[21–23]

Many solutions to the problem of oxygen have been explored, such as in situ enzymatic deoxygenation by glucose oxidase,[24–26] singlet-oxygen generation by organic[27] or organometallic[19,21,28] photocatalysts, ultra-fast initiator decomposition,[29] and sacrificial tertiary amines.[30] While these newly developed methods are effective, setup can still be complex and reagents such as enzymes and dyes are sensitive and/or expensive.

This contribution shows that well-controlled polymers can be synthesized in a minimalistic reaction setup, with only two active ingredients and no deoxygenation protocol. This work is inspired by the Haddleton group's work on low-volume oxygen-tolerant ATRP,[31,32] and the Bruns group's approach of using a layer of mineral oil.[33] In our approach, oxygen is merely excluded by filling headspace volume in the vial with an inert, immiscible liquid such as water or mineral oil (Scheme 1a, Figure S1). Polymerization is accomplished using 350nm lamps in a photoreactor, which enables homolytic cleavage of the carbon-sulfur bonds of the RAFT chain transfer agent

(CTA), allowing it to act as initiator, chain transfer agent, and reversible terminator (iniferter) (Scheme 1b).[34,35] With the elimination of headspace, only the remaining dissolved oxygen inhibits polymerization over a short induction period. The simplicity of this approach enables both hydrophilic and hydrophobic polymers to be synthesized, and the benefit is most likely to be realized when the reaction must be performed on a small scale, due to limited amounts of reagents and difficulty in accessing conventional methods of deoxygenation.

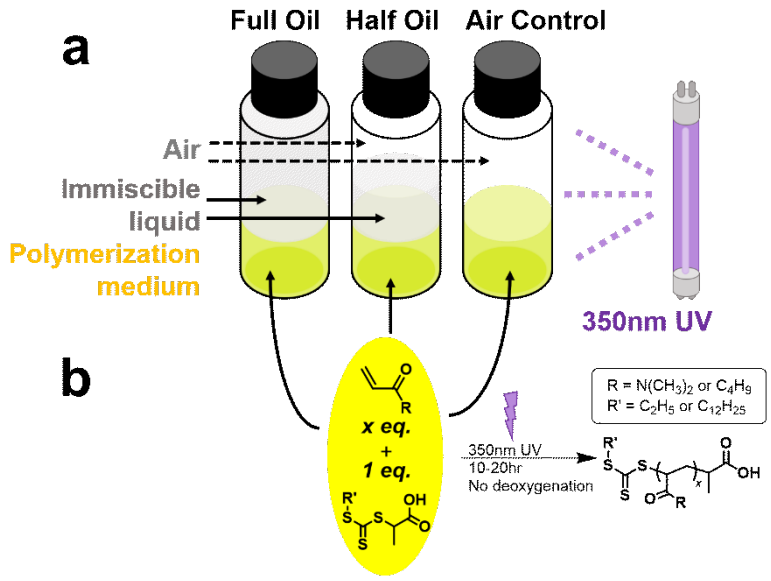

Scheme 1. (a) Vials filled with 500uL aqueous RAFT reaction mixture and varying amounts of mineral oil. Total vial volume is 1.95ml. (b) RAFT iniferter scheme. Dimethyl acrylamide (DMAm) was polymerized with the CTA PAETC and butyl acrylate (BA) was polymerized with the CTA PADTC.

Results and Discussion

Initially, photoiniferter polymerization of N,N-dimethyl acrylamide (DMAm) was performed using propionic acid ethyl trithiocarbonate (PAETC) as the CTA. DMAm is a water-soluble monomer, and hence polymerization in water was performed, with mineral oil used as an inert layer. The kinetics of DMAm polymerization targeting 100 units yielded surprising results. While we expected no conversion in the air and half-oil samples, the air sample underwent significant

conversion, and the half-oil system exhibits similar reaction rate to the air-free system ("full oil") (Fig. 1a). It is likely that the mineral oil acts as a barrier to diffusion of oxygen, causing the similar kinetics in the half and full oil systems.[33] However, in the DP50 kinetics, very small conversion is obtained in the air control (fig. 1b). Another important fact is that, even though the inert layer acts as an oxygen barrier for the polymerization mixture, it does not interfere with the NMR analysis of the polymerization mixture. As shown in the Figure 1b, 50DP kinetics displays an induction period up to 3hrs of irradiation time. The NMR of the 2hrs sample was checked for the impurities from the mineral oil (hexadecane; 1-2 ppm) since no polymer peaks will appear in that region during the induction period (Figure S2). Except for the -CH_3 peak in the CTA we did not observe any major peaks in the region where mineral oil's peaks can be found (1-2 ppm).

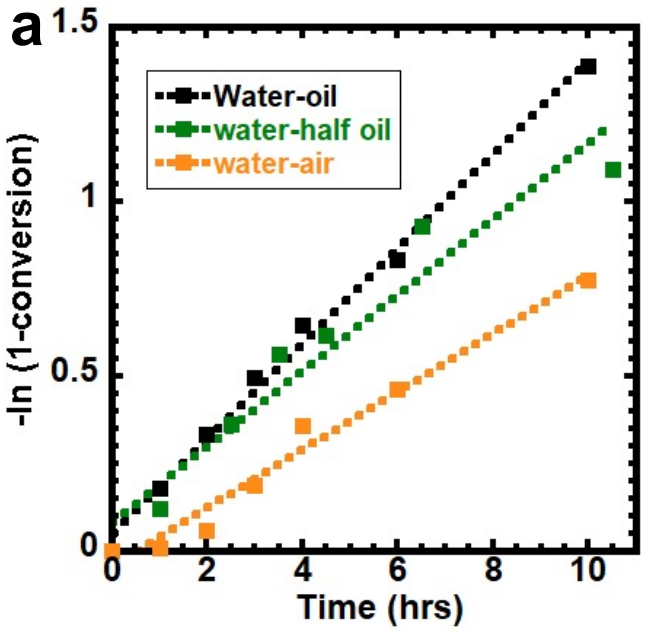

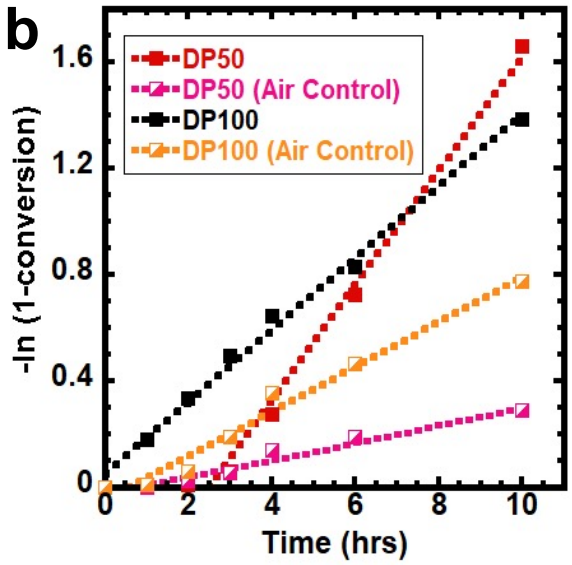

Figure 1. Photoiniferter kinetics of DMAm polymerization comparing different (a) headspace (at DP100) and (b) chain length conditions. Conditions: [DMAm] = 4.85M. [DMAm]:[PAETC]=50 or 100:1. Reaction volume = 0.5ml, with ca. 1.45ml mineral oil (full oil) or 0.75ml mineral oil (half oil). Irradiation at 350 nm with intensity of 14 ± 1 mW/cm^2.

The DP50 kinetics experiences a 3hr induction period during which dissolved oxygen is consumed and the RAFT equilibrium is established, after which the reaction proceeds at a faster rate than the DP100 system. The concentration of CTA in the DP50 system is double that of the DP100 system, which may account for the observed induction period and rate. At this concentration, the CTA is likely to be significantly reducing penetration depth of the UV light. As a result, oxygen in the interior is being consumed quite slowly, since the reaction vessel is not stirred. On the other hand, at DP100, enough UV light reaches the interior to quench all the oxygen quickly enough that no induction period is observed. Additionally, if the first monomer unit is added more slowly than subsequent units, the polymerization could be slow in the early phase. However, the steady-state

polymerization rate is higher in the DP 50 compared to the DP 100 system, because there is more UV-homolyzed CTA present overall. These initialization effects are magnified with no immiscible solvent, leading to longer induction periods when no oil is used (Fig 1b).

The SEC results for these reactions are presented in figure 2a-d. Dispersity is low over the course of reaction in most cases, although early stages of the DP100 half-oil system exhibit dispersities closer to 1.5, due to some low-MW species visible in fig. 2b, these smaller species eventually extend and the dispersity returns to 1.1-1.2. Chain growth is excellent in the DP100 full oil system (fig. 2c). The DP50 full-oil system extends well at the 4hr timepoint, but the 6hr and 10hr timepoints have very similar traces on the low-MW edge. In all cases, $M_{n,SEC}$ tracks $M_{n,Theory}$ closely.

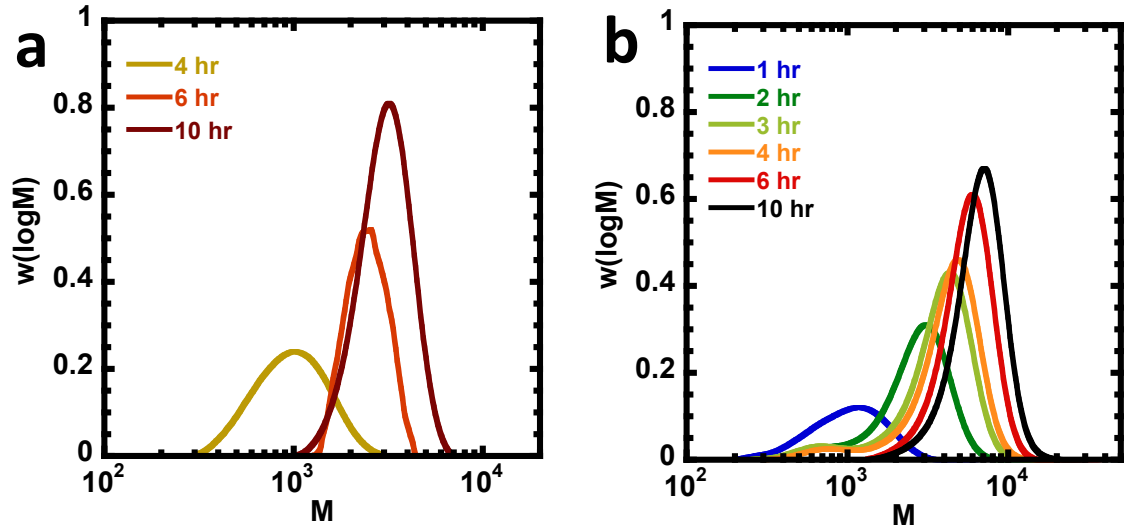

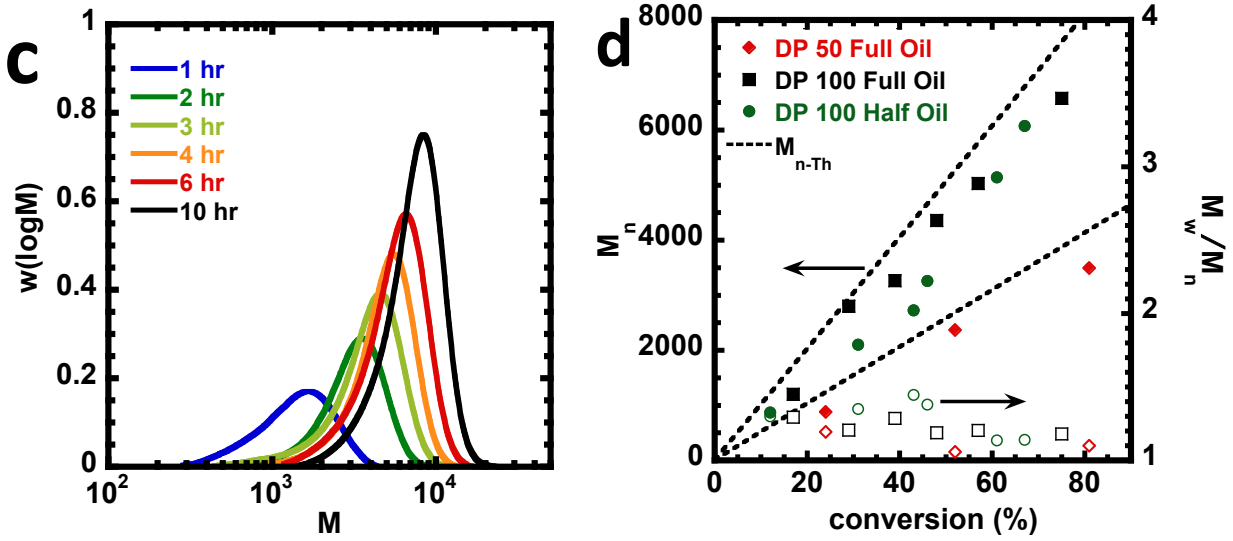

Figure 2. SEC data of iniferter reactions. (a) DP50 DMAm; (b) DP100 DMAm with less oil ("half oil"); (c) DP100 DMAm with completely filled headspace ("full oil") (peak heights normalized by conversion). (d) Procession of M_n (Black dashed lines indicate the theoretical Mn variation from DP50 and DP100) and dispersity over the course of reaction when targeting DP50 and DP100 DMAm (solid symbols indicate M_n and hollow symbols indicate M_w/M_n). Irradiation at 350 nm with intensity of 14 ± 1 mW/cm^2.

To expand on the scope of this system, polymerization in non-aqueous solvents was attempted, since acrylamides in water are sometimes considered privileged due to their unusually high k_p values in water.[36] In this case, we used butyl acrylate (BA), polymerizing in either ethyl acetate (EtOAc), which is less dense than water, or diethyl phthalate (DEP), which is more dense than water (Figure 3). In both cases the CTA used was propionic acid dodecyl trithiocarbonate (PADTC). Pleasingly, polymerization proceeds smoothly in 10 hours in both solvents, with similarly low dispersity and $M_{n,SEC}$ which is close to $M_{n,Th}$. With EtOAc as the top layer, which is in contact with the inevitable (approximately 50 μL) air bubble that remains after capping the vial (Figure S3), there was a concern that polymerization would be retarded or halted, but this does not

appear to be the case. Whatever oxygen remains in the bubble is quenched thoroughly enough that polymerization proceeds, and ultimately the polymerizations were comparable as shown in Figure 3a, although the reaction in DEP was somewhat faster than the polymerization in EtOAc. Photoiniferter polymerizations gave well controlled polymers with narrow molecular weight distributions as indicated in Figure 3b, although the system with DEP had better control over the molecular weight. Similar polymerizations were possible down to 90 μL of reaction volume as indicated in Figure S4, showing that this approach can be used to achieve microliter volume reactions. Even at these small reaction volumes, the photoiniferter process proceeded rapidly, and the resulting poly(BA) was well controlled with narrow molecular weight distributions and linear growth of M_n with conversion.

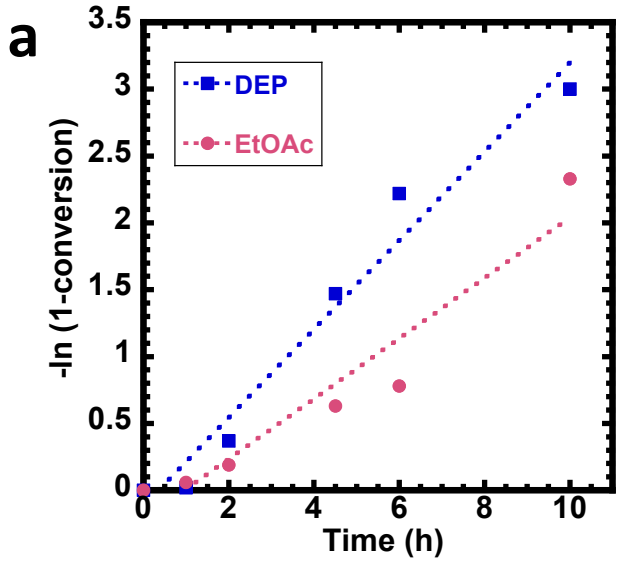

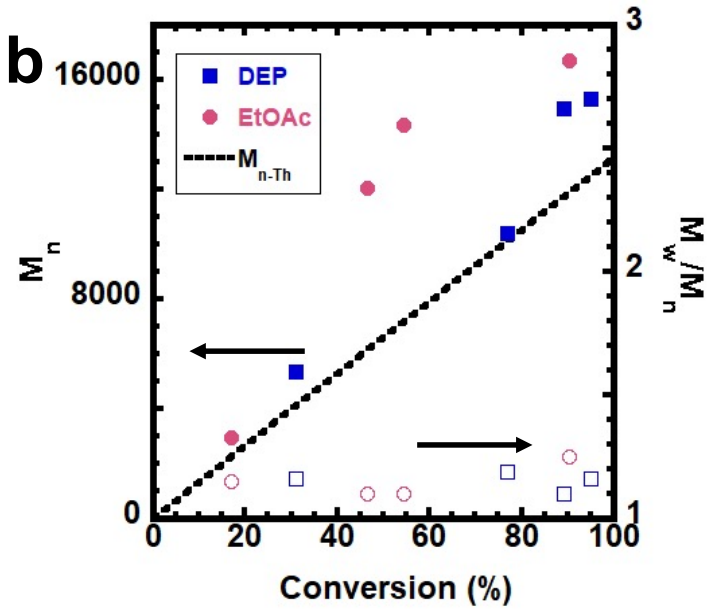

Figure 3: Photoiniferter polymerization of butyl acrylate in a reaction vessel half filled with water with the polymerization either in ethyl acetate (EtOAc) or diethylphthalate (DEP). Conditions [BA]:[PADTC]=100:1. [BA] = 3.5M. Reaction volume = 0.5ml, with ca. 1.45ml water as inert solvent. (a) gives the semilogarithmic polymerization kinetics and (b) shows the evolution of M_n (Black dashed line indicates the theoretical Mn variation) and M_w/M_n with conversion (solid symbols indicate M_n and hollow symbols indicate M_w/M_n). Irradiation at 350 nm with intensity of 14 ± 1 mW/cm^2 .

To further explore the potential of these iniferter systems to make complex polymers a sequential block copolymerization strategy was designed. In this system, photoiniferter reactions of hydrophobic monomers in DEP as the solvent were used. The remainder of the reaction volume was occupied with water. The advantage of this approach was that as more monomer is added to make subsequent blocks, the water is displaced. This offers a possible advantage over a fully filled vial approach, since the inert solvent is removed at each block addition. Cloudiness in the top/inert/water layer is observed due to some mixing at the interface; small amounts of monomer

presumably diffuse into the water layer and polymerize to form light scattering nanoparticles. This filling of the vial with new monomer is demonstrated in Figure 4a. As shown in Figure 4b, complex triblock copolymers could be synthesized using a sequential approach. Photoiniferter polymerization of the first BA block was run for 10 h reaching over 95% conversion and yielding a well-controlled polymer as shown in Figure 4b. This poly(BA) macroCTA was chain extended with 50 units of ethyl acrylate (EA) reaching over 95% conversion in 10 h. The formation of a block copolymer was evidenced by the clear shift of the SEC derived molecular weight distribution in Figure 4b. Finally, a triblock copolymer was formed by adding an additional 50 units of butyl acrylate, reaching 90% conversion in 12 h. The triblock copolymer was evidenced by the shift from the poly(BA-b-EA) macroCTA to the complex poly(BA-b-EA-b-BA) triblock copolymer. The dispersities of the polymers were M_w/M_n=1.11 for the poly(BA), M_w/M_n=1.11 for the poly(BA-b-EA) and M_w/M_n=1.24 for the poly(BA-b-EA-b-BA) material.

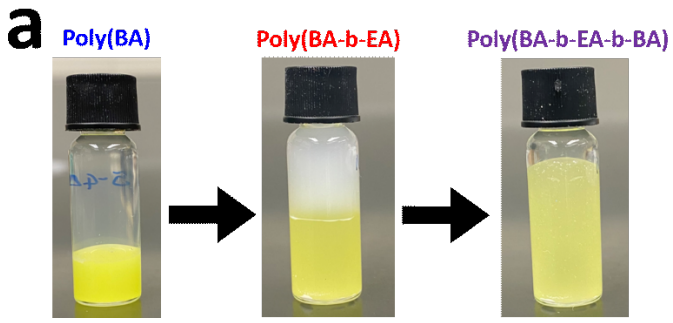

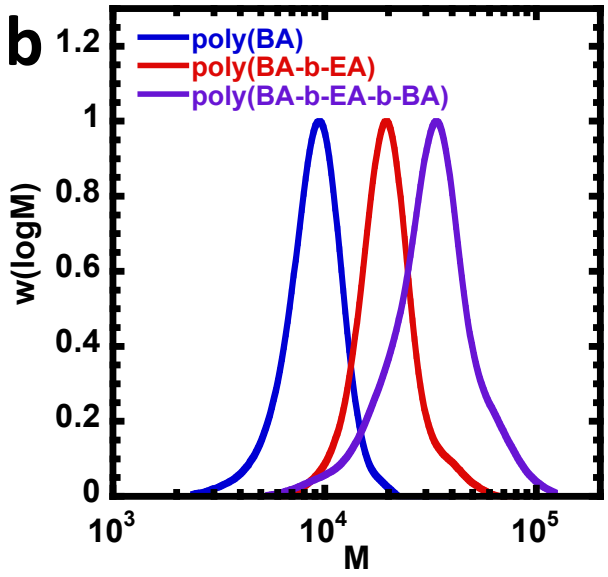

Figure 4. Block copolymerization of hydrophobic monomers BA and EA using DEP as the solvent. (a) the sequential filling of the vial by subsequent monomer additions. (b) SEC derived molecular weight distributions poly(BA), poly(BA-b-EA) , and poly(BA-b-EA-b-BA). Each block was polymerized using a ratio of [BA] or [EA]: [ ] = 50: 1. The first block was polymerized using PADTC as the CTA. Irradiation at 350 nm with intensity of 14 ± 1 mW/cm^2.

Intrigued by the idea that this method could restrict polymerization to just one layer of a two-layer system, gradient polymerization was attempted. While gradient character can be achieved using continuous feed and other methods,[37,38,38,39] this system could be simpler and require no special equipment other than the UV reactor. In this system, NiPAm and DMAm were co-polymerized with a toluene layer and an aqueous layer, as shown in Scheme 2. Due to differing partition coefficients, NiPAm begins with a concentration of around 0.67:1 versus DMAm, corresponding to a DMAm fraction in the aqueous phase of approximately 0.6. PAETC is confined to the aqueous layer by addition of NaOH.

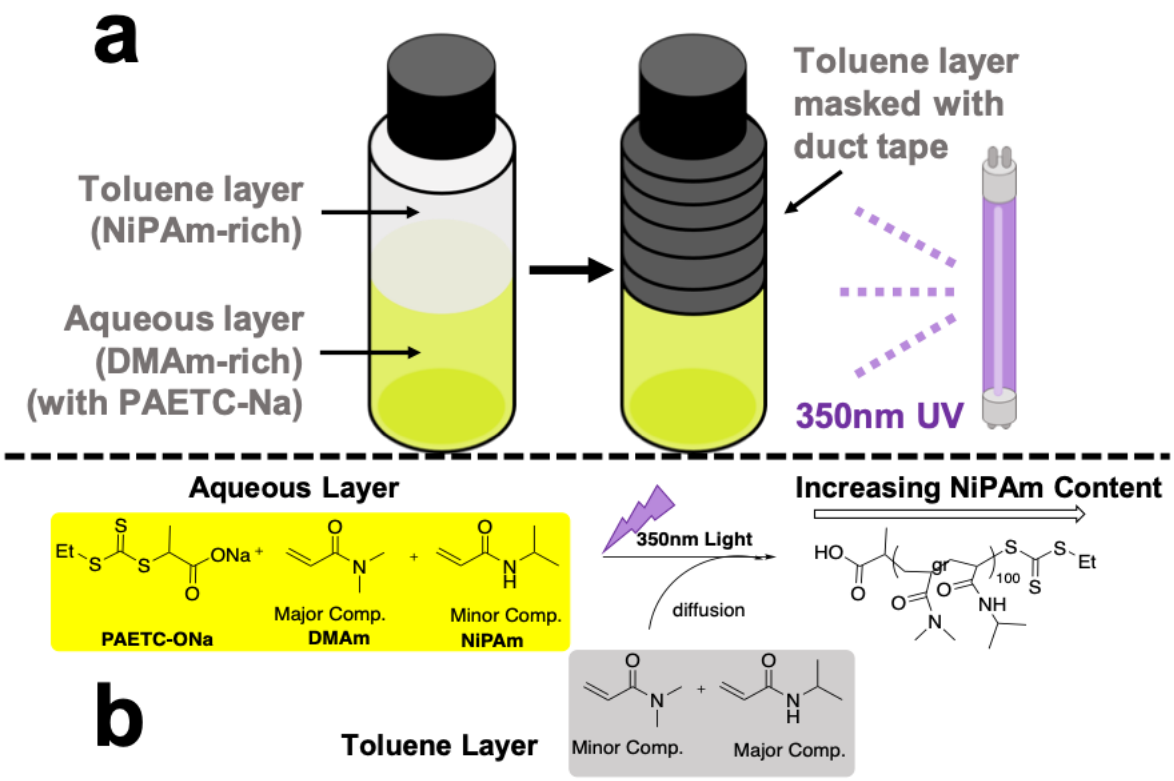

Scheme 2. (a) Schematic representation of gradient experimental setup, where the NiPAm-rich toluene layer is masked with duct tape. PAETC is confined to the aqueous layer by addition of NaOH. (b) Scheme showing diffusion-controlled gradient polymerization of DMAm and NiPAm.

The kinetics of both DMAm and NiPAm polymerization in the aqueous phase were very similar, reaching essentially quantitative conversion after 24h. This is shown in Figure 5a. Although the monomers present in the aqueous phase polymerize at similar rates, regardless of whether they are NiPAm or DMAm, the fraction of DMAm and NiPAm changes over the course of the reaction. Initially the aqueous reaction phase is rich in DMAm, as it is the more polar monomer, being close

to 70% DMAm+poly(DMAm) at 2h. As the reaction progresses, NiPAm transfers into the aqueous phase from the organic toluene phase. After 24h, where the conversion is close to 100%, the polymer contains close to the targeted 50% DMAm and NiPAm, as shown in Figure 5b. The resulting polymers are monomodal with Mn of 9,900 close to the targeted Mn of 10,600, although the final polymer reaches a moderate dispersity of 1.5. Despite the high dispersity, this approach enables a unique approach to gradient synthesis with tolerance to oxygen.

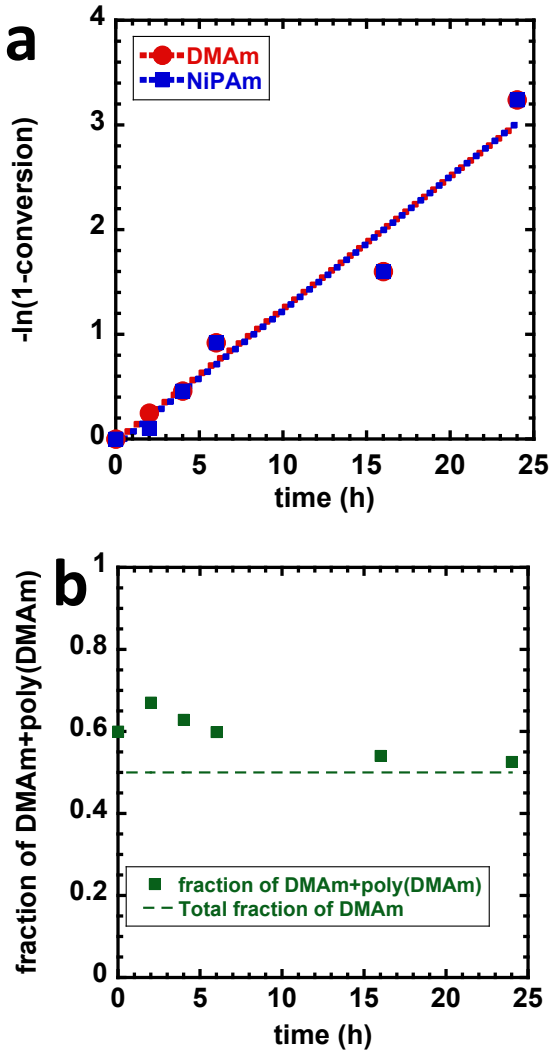

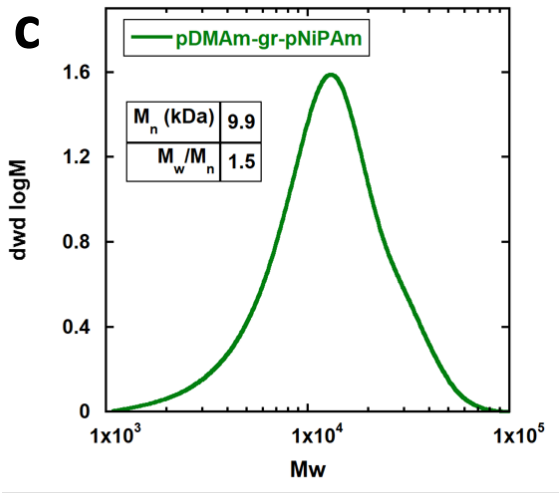

Figure 5: (a) Semilogarithmic plot of gradient polymer formation for both NiPAm and DMAm in the aqueous phase. (b) Ratio of total dimethylacrylamide (both monomer and polymerized) to all monomer and polymer in the aqueous phase. (c) SEC derived molecular weight distribution of the final gradient copolymer.

Conclusions

In this work, a simple and robust approach to tailored polymers is explored. Combining the photoiniferter process with a no-headspace experimental setup, tailored polymers of hydrophobic and hydrophilic monomers, including block and gradient copolymers, were obtained. Hydrophilic DMAm polymers were synthesized using mineral oil as an inert liquid to fill the vial headspace and effectively reduce oxygen content, while hydrophobic BA polymers were synthesized using water as inert liquid. In both cases, high conversion and low dispersities were observed. This method scales down well, as good conversion and dispersity were seen for BA polymerization in volumes as low as 90µl. Block polymers of BA and EA were accessible with this approach in a highly simplified manner - excess water could simply be displaced as more monomer was added in each chain extension step. Finally, gradient copolymers of DMAm and NiPAm were obtained

by using partition coefficients and diffusion to control monomer feeding over the course of polymerization. While the dispersity of the gradient copolymer is modest (1.5), further improvements could be made in the future by altering conditions such as concentration and cosolvents. In summary, this method can be used to make a variety of tailored polymers with advantages of safety and simplicity: safety, by avoiding needles (for gas sparging), radical initiators, and high temperatures; and simplicity, by requiring fewer ingredients in the experimental setup, minimal instrumentation, no inert gases, and mass-produced vials. As a result of its simplicity and tolerance to low volumes, this method is also economical and suited to production of polymer libraries.

Acknowledgements

This work was partially supported by the National Science Foundation under Grant No. (DMR-2030567). 400 MHz NMR instrumentation is supported through funding from the National Science Foundation under grant number (CHE- 1919850) D.K. acknowledge support from Miami University through startup funding and the Robert H. and Nancy J, Blayney Professorship.

References

(1) Parkatzidis, K.; Wang, H. S.; Truong, N. P.; Anastasaki, A. Recent Developments and Future Challenges in Controlled Radical Polymerization: A 2020 Update. *Chem* **2020**, *6* (7), 1575–1588. https://doi.org/10.1016/j.chempr.2020.06.014.

(2) Ribelli, T. G.; Lorandi, F.; Fantin, M.; Matyjaszewski, K. Atom Transfer Radical Polymerization: Billion Times More Active Catalysts and New Initiation Systems. *Macromol. Rapid Commun.* **2019**, *40* (1), 1800616. https://doi.org/10.1002/marc.201800616.

(3) Aklujkar, P. S.; Rao, A. R. Developments in the Components of Metal-Free Photoinitiated Organocatalyzed-Atom Transfer Radical Polymerization (O-ATRP). *ChemistrySelect* **2020**, *5* (47), 14884–14899. https://doi.org/10.1002/slct.202004194.

(4) Wang, Y.; Nguyen, M.; Gildersleeve, A. J. Macromolecular Engineering by Applying Concurrent Reactions with ATRP. *Polymers (Basel).* **2020**, *12* (8), 1706. https://doi.org/10.3390/polym12081706.

(5) Jumeaux, C.; Chapman, R.; Chandrawati, R.; Stevens, M. M. Synthesis and Self-Assembly of Temperature-Responsive Copolymers Based on N-Vinylpyrrolidone and Triethylene Glycol Methacrylate. *Polym. Chem.* **2015**, *6* (22), 4116–4122. https://doi.org/10.1039/C5PY00483G.

(6) Zavada, S. R.; Battsengel, T.; Scott, T. F. Radical-Mediated Enzymatic Polymerizations. *Int. J. Mol. Sci.* **2016**, *17* (2). https://doi.org/10.3390/ijms17020195.

(7) Moad, G.; Rizzardo, E. A 20th Anniversary Perspective on the Life of RAFT (RAFT Coming of Age). *Polym. Int.* **2020**, *69* (8), 658–661. https://doi.org/10.1002/pi.5944.

(8) Matyjaszewski, K. Discovery of the RAFT Process and Its Impact on Radical Polymerization. *Macromolecules* **2020**, *53* (2), 495–497. https://doi.org/10.1021/acs.macromol.9b02054.

(9) An, Z. 100th Anniversary of Macromolecular Science Viewpoint: Achieving Ultrahigh Molecular Weights with Reversible Deactivation Radical Polymerization. *ACS Macro Lett.* **2020**, *9* (3), 350–357. https://doi.org/10.1021/acsmacrolett.0c00043.

(10) Li, S.; Han, G.; Zhang, W. Photoregulated Reversible Addition–Fragmentation Chain

Transfer (RAFT) Polymerization. *Polym. Chem.* **2020**, *11* (11), 1830–1844. https://doi.org/10.1039/D0PY00054J.

(11) Li, S.; Han, G.; Zhang, W. Cross-Linking Approaches for Block Copolymer Nano-Assemblies via RAFT-Mediated Polymerization-Induced Self-Assembly. *Polym. Chem.* **2020**, *11* (29), 4681–4692. https://doi.org/10.1039/D0PY00627K.

(12) Zard, S. Z. Discovery of the RAFT/MADIX Process: Mechanistic Insights and Polymer Chemistry Implications. *Macromolecules* **2020**, *53* (19), 8144–8159. https://doi.org/10.1021/acs.macromol.0c01441.

(13) Collins, J.; McKenzie, T. G.; Nothling, M. D.; Allison-Logan, S.; Ashokkumar, M.; Qiao, G. G. Sonochemically Initiated RAFT Polymerization in Organic Solvents. *Macromolecules* **2019**, *52* (1), 185–195. https://doi.org/10.1021/acs.macromol.8b01845.

(14) Semsarilar, M.; Abetz, V. Polymerizations by RAFT: Developments of the Technique and Its Application in the Synthesis of Tailored (Co)Polymers. *Macromol. Chem. Phys.* **2021**, *222* (1), 2000311. https://doi.org/10.1002/macp.202000311.

(15) Phommalysack-Lovan, J.; Chu, Y.; Boyer, C.; Xu, J. PET-RAFT Polymerisation: Towards Green and Precision Polymer Manufacturing. *Chem. Commun.* **2018**, *54* (50), 6591–6606. https://doi.org/10.1039/C8CC02783H.

(16) Allegrezza, M. L.; Konkolewicz, D. PET-RAFT Polymerization: Mechanistic Perspectives for Future Materials. *ACS Macro Lett.* **2021**, *10* (4), 433–446. https://doi.org/10.1021/acsmacrolett.1c00046.

(17) Gormley, A. J.; Yeow, J.; Ng, G.; Conway, Ó.; Boyer, C.; Chapman, R. An Oxygen-

Tolerant PET-RAFT Polymerization for Screening Structure-Activity Relationships. *Angew. Chemie Int. Ed.* **2018**, *57* (6), 1557–1562. https://doi.org/10.1002/anie.201711044.

(18) Yeow, J.; Joshi, S.; Chapman, R.; Boyer, C. A Self-Reporting Photocatalyst for Online Fluorescence Monitoring of High Throughput RAFT Polymerization. *Angew. Chemie Int. Ed.* **2018**, *57* (32), 10102–10106. https://doi.org/10.1002/anie.201802992.

(19) Ng, G.; Yeow, J.; Chapman, R.; Isahak, N.; Wolvetang, E.; Cooper-White, J. J.; Boyer, C. Pushing the Limits of High Throughput PET-RAFT Polymerization. *Macromolecules* **2018**, *51* (19), 7600–7607. https://doi.org/10.1021/acs.macromol.8b01600.

(20) Yeow, J.; Chapman, R.; Gormley, A. J.; Boyer, C. Up in the Air: Oxygen Tolerance in Controlled/Living Radical Polymerisation. *Chemical Society Reviews*. Royal Society of Chemistry June 21, 2018, pp 4357–4387. https://doi.org/10.1039/c7cs00587c.

(21) Gormley, A. J.; Yeow, J.; Ng, G.; Conway, Ó.; Boyer, C.; Chapman, R. An Oxygen-Tolerant PET-RAFT Polymerization for Screening Structure-Activity Relationships. *Angew. Chemie* **2018**, *130* (6), 1573–1578. https://doi.org/10.1002/ange.201711044.

(22) Richards, S.-J.; Jones, A.; Tomás, R. M. F.; Gibson, M. I. Photochemical "In-Air" Combinatorial Discovery of Antimicrobial Co-Polymers. *Chem. - A Eur. J.* **2018**, *24* (52), 13758–13761. https://doi.org/10.1002/chem.201802594.

(23) Pan, X.; Lathwal, S.; Mack, S.; Yan, J.; Das, S. R.; Matyjaszewski, K. Automated Synthesis of Well-Defined Polymers and Biohybrids by Atom Transfer Radical Polymerization Using a DNA Synthesizer. *Angew. Chemie Int. Ed.* **2017**, *56* (10), 2740–2743. https://doi.org/10.1002/anie.201611567.

(24) Lv, Y.; Liu, Z.; Zhu, A.; An, Z. Glucose Oxidase Deoxygenation−redox Initiation for RAFT Polymerization in Air. *J. Polym. Sci. Part A Polym. Chem.* **2017**, *55* (1), 164–174. https://doi.org/10.1002/pola.28380.

(25) Schneiderman, D. K.; Ting, J. M.; Purchel, A. A.; Miranda, R.; Tirrell, M. V.; Reineke, T. M.; Rowan, S. J. Open-to-Air RAFT Polymerization in Complex Solvents: From Whisky to Fermentation Broth. *ACS Macro Lett.* **2018**, *7* (4), 406–411. https://doi.org/10.1021/acsmacrolett.8b00069.

(26) Ishizuka, F.; Chapman, R.; Kuchel, R. P.; Coureault, M.; Zetterlund, P. B.; Stenzel, M. H. Polymeric Nanocapsules for Enzyme Stabilization in Organic Solvents. *Macromolecules* **2018**, *51* (2), 438–446. https://doi.org/10.1021/acs.macromol.7b02377.

(27) Shih, H.; Lin, C.-C. Visible-Light-Mediated Thiol-Ene Hydrogelation Using Eosin-Y as the Only Photoinitiator. *Macromol. Rapid Commun.* **2013**, *34* (3), 269–273. https://doi.org/10.1002/marc.201200605.

(28) Li, Z.; Ganda, S.; Melodia, D.; Boyer, C.; Chapman, R. Well-Defined Polymers for Nonchemistry Laboratories Using Oxygen Tolerant Controlled Radical Polymerization. *J. Chem. Educ.* **2020**, *97* (2), 549–556. https://doi.org/10.1021/acs.jchemed.9b00922.

(29) Gurnani, P.; Floyd, T.; Tanaka, J.; Stubbs, C.; Lester, D.; Sanchez-Cano, C.; Perrier, S. PCR-RAFT: Rapid High Throughput Oxygen Tolerant RAFT Polymer Synthesis in a Biology Laboratory. *Polym. Chem.* **2020**, *11* (6), 1230–1236. https://doi.org/10.1039/c9py01521c.

(30) Fu, Q.; Xie, K.; McKenzie, T. G.; Qiao, G. G. Trithiocarbonates as Intrinsic Photoredox Catalysts and RAFT Agents for Oxygen Tolerant Controlled Radical Polymerization.

Polym. Chem. **2017**, *8* (9), 1519–1526. https://doi.org/10.1039/c6py01994c.

(31) Liarou, E.; Anastasaki, A.; Whitfield, R.; Iacono, C. E.; Patias, G.; Engelis, N. G.; Marathianos, A.; Jones, G. R.; Haddleton, D. M. Ultra-Low Volume Oxygen Tolerant Photoinduced Cu-RDRP. *Polym. Chem.* **2019**, *10* (8), 963–971. https://doi.org/10.1039/c8py01720d.

(32) Liarou, E.; Whitfield, R.; Anastasaki, A.; Engelis, N. G.; Jones, G. R.; Velonia, K.; Haddleton, D. M. Copper-Mediated Polymerization without External Deoxygenation or Oxygen Scavengers. *Angew. Chemie - Int. Ed.* **2018**, *57* (29), 8998–9002. https://doi.org/10.1002/anie.201804205.

(33) Rifaie-Graham, O.; Pollard, J.; Raccio, S.; Balog, S.; Rusch, S.; Hernández-Castañeda, M. A.; Mantel, P.-Y.; Beck, H.-P.; Bruns, N. Hemozoin-Catalyzed Precipitation Polymerization as an Assay for Malaria Diagnosis. *Nat. Commun.* **2019**, *10* (1), 1369. https://doi.org/10.1038/s41467-019-09122-z.

(34) Burridge, K. M.; Wright, T. A.; Page, R. C.; Konkolewicz, D. Photochemistry for Well-Defined Polymers in Aqueous Media: From Fundamentals to Polymer Nanoparticles to Bioconjugates. *Macromol. Rapid Commun.* **2018**, *39* (12), 1800093–1800114. https://doi.org/10.1002/marc.201800093.

(35) McKenzie, T. G.; Fu, Q.; Uchiyama, M.; Satoh, K.; Xu, J.; Boyer, C.; Kamigaito, M.; Qiao, G. G. Beyond Traditional RAFT: Alternative Activation of Thiocarbonylthio Compounds for Controlled Polymerization. *Adv. Sci.* **2016**, *3* (9). https://doi.org/10.1002/advs.201500394.

(36) Carmean, R. N.; Becker, T. E.; Sims, M. B.; Sumerlin, B. S. Ultra-High Molecular Weights

via Aqueous Reversible-Deactivation Radical Polymerization. *Chem* **2017**, *2* (1), 93–101. https://doi.org/10.1016/j.chempr.2016.12.007.

(37) Guo, Y.; Zhang, J.; Xie, P.; Gao, X.; Luo, Y. Tailor-Made Compositional Gradient Copolymer by a Many-Shot RAFT Emulsion Polymerization Method. *Polym. Chem.* **2014**, *5* (10), 3363–3371. https://doi.org/10.1039/C4PY00003J.

(38) Zheng, Z.; Gao, X.; Luo, Y.; Zhu, S. Employing Gradient Copolymer To Achieve Gel Polymer Electrolytes with High Ionic Conductivity. *Macromolecules* **2016**, *49* (6), 2179–2188. https://doi.org/10.1021/acs.macromol.6b00021.

(39) Zhou, Y.-N.; Li, J.-J.; Luo, Z.-H. Synthesis of Gradient Copolymers with Simultaneously Tailor-Made Chain Composition Distribution and Glass Transition Temperature by Semibatch ATRP: From Modeling to Application. *J. Polym. Sci. Part A Polym. Chem.* **2012**, *50* (15), 3052–3066. https://doi.org/10.1002/pola.26091.

Graphical TOC Entry